Biomechanical cyclic loading test of a synthetic ligament fixation system used for intra-articular stabilization of deficient canine stifles

Bastien Goin, Philippe Buttin, Yoann Lafon, Michel Massenzio, Eric Viguier, Thibaut Cachon

Open Veterinary Journal, (2022), Vol. 12(3): 341–350
ISSN: 2226-4485 (Print)
ISSN: 2218-6050 (Online)

Original Research
DOI: *10.5455/OVJ.2022.v12.i3.6*

Submitted: 21/01/2022 Accepted: 04/05/2022 Published: 29/05/2022

Biomechanical cyclic loading test of a synthetic ligament fixation system used for intra-articular stabilization of deficient canine stifles

Bastien Goin[1,2,3], Philippe Buttin[4], Yoann Lafon[2], Michel Massenzio[2], Eric Viguier[1] and Thibaut Cachon[1*]

[1]*Université de Lyon, VetAgro Sup, Interactions Cellules Environnement (ICE), Lyon, France*
[2]*Univ Lyon, Univ Gustave Eiffel, Univ Claude Bernard Lyon 1, LBMC UMR T_9406, F-69622 Lyon, France*
[3]*Novetech Surgery, Monaco, Monaco*
[4]*Itinerant surgeon, Villaz, France*

Abstract

Background: Cranial cruciate ligament rupture (CCLr) is the most common cause of hind limb lameness in dogs. Currently, surgical management of CCLr is mostly performed using tibial osteotomy techniques to modify the biomechanical conformation of the affected stifle. These surgical techniques have a significant complication rate, associated with persistent instability of the stifle which may lead to chronic postoperative pain. Over the last decade, studies have been published on various techniques of anatomical caudal cruciate ligament reconstruction in veterinary practice, using physiological autografts or woven synthetic implants.

Aim: The aim of this *ex vivo* biomechanical study is to investigate the *ex vivo* dynamic biomechanical behavior of a synthetic implant ultrahigh molecular weight polyethylene (UHMWPE) implant fixed with interference screws for the treatment of CCLr in dogs, according to a fatigue protocol (48 hours per test).

Methods: Seven stifles from four skeletally mature canine cadavers were implanted with the synthetic implant. It was fixed with four interference screws inserted in transversal and oblique tunnels in both the distal femur and the proximal tibia. For each case, 100,000 cycles were performed at 0.58 Hz, with traction loads ranging from 100 to 210 N.

Results: Neither screw-bone assembly rupture nor a pull-out issue was observed during the dynamic tests. Linear stiffness of the implants associated with a fixation system with four interference screws increased over time. The final displacement did not exceed 3 mm for five of the seven specimens. Five of the seven synthetic implants yielded to a lengthening in functional range (0–3 mm). Linear stiffness was homogeneous among samples, showing a strong dynamic strength of the interference screw-based fixations of the UHMWPE implant in the femoral and tibial bones.

Conclusion: This study completes the existing literature on the biomechanical evaluation of passive stifle stabilization techniques with a testing protocol focused on cyclic loading at a given force level instead of driven by displacement. These biomechanical results should revive interest in intra-articular reconstruction after rupture of the CCLr in dogs.

Keywords: Biomechanical analysis, Cranial cruciate ligament, Synthetic ligament reconstruction, UHMWPE implant, Dog.

Introduction

Cranial cruciate ligament rupture (CCLr) is the most common hind limb pathology in dogs with an estimated prevalence of 4.87% (Witsberger *et al.*, 2008). The treatment involves surgery and cost 1.32 billion dollars in the USA in 2003 (Wilke *et al.*, 2005). Total rupture of the caudal cruciate ligament (CCL) induces a cranio-caudal and internal rotation (pivot shift) instability of the tibia. It triggers severe lameness and pain and leads to an osteoarthritic process requiring surgery (Baird *et al.*, 1998). The aim of this surgical procedure is to stabilize the stifle by removing the cranial drawer motion (Johnson and Johnson, 1993). There are two types of strategies:

– active stabilization by osteotomy of the tibia, thus changing the biomechanical conformation of the stifle. This surgery aims at suppressing the biomechanical role of the CCL in the craniocaudal stabilization of the stifle (Kim *et al.*, 2008).
– passive stabilization, which does not require any biomechanical modification of the articulation. It aims at stabilizing the stifle with synthetic implants respecting the anatomical physiology.

Such implants can be implanted either (i) extra-articularly as in the FLO (1975) or the TightRope (TR) (Cook *et al.*, 2010) techniques; or (ii) intra-articularly as introduced recently by Barnhart *et al.* (2016) and several other authors (Cook *et al.*, 2017; Prada *et al.*, 2018) for synthetic implants, or by Biskup and Conzemius (2020) for intra-articular allografts. Unfortunately, in human anterior cruciate ligament (ACL) surgery, synthetic intra-articular techniques have failed several times in the last quarter of the 20th century (Legnani *et al.*, 2010). The use of autogenous graft tissue has always been a widely accepted method of restoring the function of knees affected by cruciate ligament deficiency (Salmon *et al.*, 2006; Hui *et al.*, 2011). Over the two last decades, synthetic ligament

***Corresponding Author:** Thibaut Cachon. Université de Lyon, VetAgro Sup, Interactions Cellules Environnement (ICE), Lyon, France. Email: *thibaut.cachon@vetagro-sup.fr*

implants have won acclaim, thanks to the Ligament Augmentation and Reconstruction System (LARS) techniques (Gao *et al.*, 2010), known as a possible alternative to autogenous graft techniques for surgical management of the human ACL rupture.

According to this recent trend, brand new intra-articular devices have been developed for passive stabilization of the stifle, composed of an ultrahigh molecular weight polyethylene (UHMWPE) artificial ligament fixed on the bones with interference screws (Blanc *et al.*, 2019; Goin *et al.*, 2019; Rafael *et al.*, 2020). This approach seems to be spreading among the international veterinary community (Barnhart *et al.*, 2016; Cook *et al.*, 2017; Barnhart *et al.*, 2018; Prada *et al.*, 2018; Barnhart *et al*., 2019; Biskup and Conzemius, 2020), although it remains marginal in the treatment of CCL rupture (von Pfeil *et al.*, 2018). The objective of this study is to evaluate the biomechanical behavior of this new artificial ligament implanted in *ex vivo* stifles under cyclic tensile tests.

Material and Methods

Sample acquisition and preparation protocol

All anatomical parts came from euthanized dogs for reasons unrelated to the focus of this study, belonging to the refuge of the Society for the Protection of Animals (SPA) in Lyon. This anonymized cadaver donation process between the SPA and VetAgro Sup was sealed by an agreement. Seven hind limbs were collected on the cadavers of freshly frozen mature dogs weighing between 25 and 35 kg. All dogs were similar in size. The stifles were dissected to reveal the tibia, the meniscus, and the femur. Stifles that were free of osteoarthritis and with no ligamentous and meniscal lesions were kept for study purposes. The proximal extremity of the femur and the distal extremity of the tibia were inserted into square metal plots (30 × 30 × 70 mm) with polymethyl methacrylate to secure the fixation of the bone extremities in the testing machine. A total of seven distinct tests were conducted with the following nomenclature: 1D, 1G, 2G, 3D, 3G, 4D, and 4G. The first number refers to the dog from which the samples were taken. Letters "D" and "G" stand for right and left laterality, respectively.

Description of the medical device

The brand new intra-articular UHMWPE device tested in this study is the Novalig 8000 implant (Novetech Surgery, Monaco). It is made of medical-grade UHMWPE monofilaments braided and woven in a specific way (Fig. 1). It has two components: a puller wire allowing the insertion of the implant into the bone tunnels (Fig. 1a) and the intra-articular functional section (Fig. 1b) secured by interference screws. The manufacturer reports a strong biomechanical resistance to traction strengths higher than the physiological CCL by more than 8,000 N (Butler *et al.*, 1983; Patterson *et al.*, 1991). Based on state-of-the-art biomechanical tests carried out on this intra-articular reconstruction technique of the CCL, no implant rupture was reported

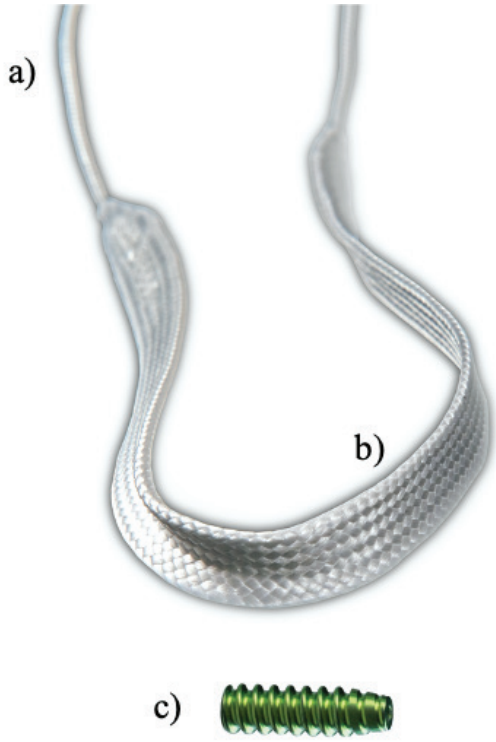

Fig. 1. UHMWPE implant. (a) Puller wire section. (b) Intra-articular functional section secured by (c) interference screw.

in quasi-static pull-out tests (Blanc *et al.*, 2019) or in cyclic loading tests (Goin *et al.*, 2019), with a maximum resistance before implant slippage estimated at 690 ± 115 N. The synthetic ligament was sterilized with ethylene oxide and implanted with four titanium interference screws (diameter: 4.5 mm; length: 20 mm) provided by the same implant manufacturer (Fig. 1c).

Implantation procedure

The samples were thawed at room temperature for 24 hours. They were implanted with the UHMWPE synthetic implant according to the recommended "Out-In" surgical procedure, in which interference screws are implanted from the epiphyseal surface of the femur and the tibia toward the intra-articular space (Blanc *et al.*, 2019). Once the CCL was entirely resected, the implantation was performed on specific anatomical regions of the *in vivo* CCL insertion to ensure its physiological reconstruction. The whole implantation procedure was performed with the cadaveric stifles placed in hyperflexion. A first oblique femoral tunnel was drilled (Fig. 2) from the caudolateral insertion of the CCL by means of an ancillary device provided in the implantation kit. Another oblique tibial tunnel was drilled from the tibial cranio-medial insertion of the CCL. The UHMWPE implant was then inserted through these two tunnels using a needle threader. One interference screw was inserted in the first tunnel from the outside to the inside of the distolateral face of the femoral metaphysis. All screws were 4.5 mm

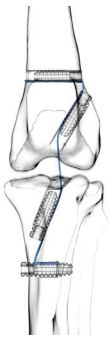

Fig. 2. Schematic view of synthetic intra-articular CCL reconstruction fixed by four interference screws.

wide and 20 mm long. A transversal tunnel was drilled through the distal metaphysis of the femur at 10 mm from the proximal output of the first tunnel. Once the implant was passed through this third tunnel, again using a needle threader, a second interference screw was inserted in the pre-threaded tunnel from the lateral to the medial faces of the femur. Another screw was implanted in the previously threaded oblique tibial tunnel from the outside in, while maintaining the prosthesis under tension. A final transversal tunnel was drilled in the proximal metaphysis of the tibia, 10 mm away from the distal output of the second tunnel. The UHMWPE implant was passed through this tunnel with a needle threader and a fourth interference screw was inserted from the medial to the lateral faces of the tibia (Fig. 3). After implantation, the clinician checked for the absence of cranial drawer motion to confirm that the procedure was successful.

Biomechanical testing

The stifle joints reconstructed with the UHMWPE implant fixed by the interference screw technique were tested biomechanically under uniaxial tensile cyclic loading. These trials were conducted at room temperature (23°C) (Cocca *et al.*, 2020) on seven implanted stifles using a traction testing machine (AGS-X Shimadzu, Japan). Each implanted *ex vivo* specimen was initially positioned at 180° to ensure the alignment of both the femoral and tibial oblique tunnels, and therefore the reproducibility of the initial boundary conditions of the protocol (Fig. 4a). The physiological environment was kept close to reality by using sterile compresses moistened with physiological saline applied directly on the surface of the anatomical pieces. The compresses were maintained in place with polyethylene stretch sheets, thus guaranteeing humidity of the set-up throughout the 48-hour-long tests (Fig. 4b).

A preliminary quasi-static traction test was performed at 20 mm/minute until 100 N to preload the implanted joint and to close the gaps of the set-up. A 100,000-cycle dynamic tensile test was then conducted at a 0.58 Hz frequency for an overall duration of approximately 48 hours per specimen. This cyclic loading aims at reproducing the joint loading for an

Fig. 3. Final visualization of the surgical procedure for stifle stabilization using intra-articular synthetic implant.

animal operated with this technique but not having respected the recommended immediate postoperative resting period. The force of these dynamic tests was controlled, ranging from 100 N (minimal pre-loading) to 210 N. This is based on a previous study reporting that the ground reaction force is equal to 65% of the dog's body weight when trotting (Rumph *et al.*, 1995). Since the tested specimens were taken from 30-kg dogs on average, the ground reaction force would approximately be equal to 195 N (plus a 15 N-safety margin, yielding to a maximum load of 210 N). This loading range is coherent with *ex vivo* cyclic tests of fixation devices for human ACL reconstruction (Kousa *et al.*, 2003; Brown *et al.*, 2004). After each cyclic test, the integrity of the implanted joint was controlled by a specific X-ray exam.

Data acquisition and processing

The sensors used to record the force (5 kN load cell) and the displacement (mechanical traverse stroke) were those natively associated with the testing machine. The synchronized acquisition of the measurements was carried out using the TrapeziumX software (Shimadzu, Japan) with a sampling frequency of 10 Hz. Owing to the large number of cycles, any acquisition represents a dataset of 1.620.000 points of measurement stored in a 41.5 Mo file per test. The data were processed with Matlab® Release 2018 (The MathWorks, Inc., Natick, MA) and Excel® (Microsoft Corporation, Albuquerque, NM). Raw data were analyzed to extract several parameters from each test. Raw displacement data were filtered by applying a two-way average moving filter (window size: $N = 500$ over approximately 30 cycles) to extract the global behavior of each tested sample (mean filtered displacement curves). The displacement of the traverse stroke was recorded. Linear stiffness was computed on several cycles (1st, 2nd, 10th, and

100,000th ones) as the slope of the load–displacement curve in the given cycle interval to illustrate a potential stress softening effect (Fig. 5).

All the statistics were performed with Statext ver. 3.3 (STATEXT LLC, Wayne, NJ, USA), using a 5% significance level.

Ethical approval

Not applicable for this study: "All anatomical parts came from euthanized dogs for reasons unrelated to the focus of this study, belonging to the refuge of the SPA in Lyon. This anonymized cadaver donation process between the SPA and VetAgro Sup was sealed by an agreement."

Results

Neither screw-bone assembly rupture nor a pull-out issue was observed during the dynamic tests (Fig. 6). All mean filtered displacement curves had a similar

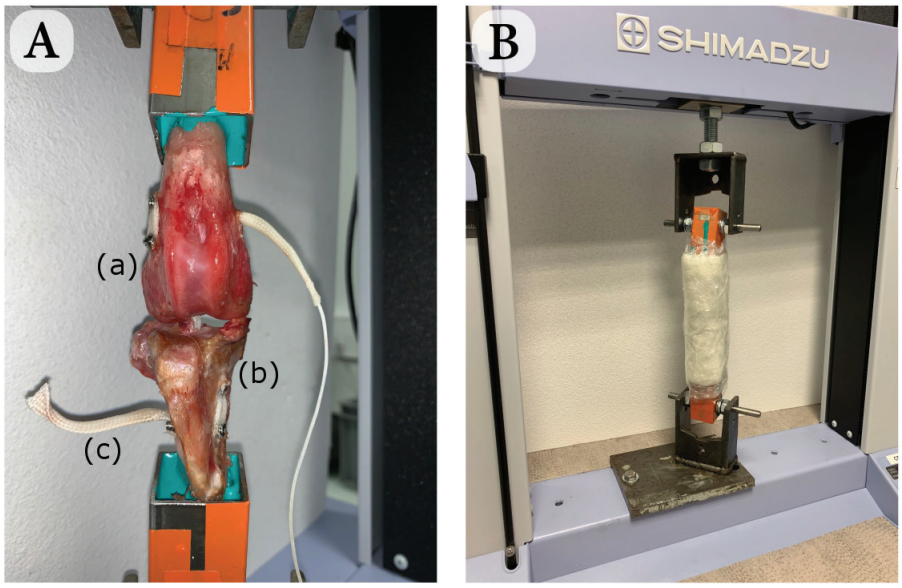

Fig. 4. (A) Experimental set-up after UHMWPE implant was implanted (intra-articular implant) with four interference screws: (a) femur, (b) tibia, and (c) UHMWPE implant. (B) Test with traction machine. Moistened compresses around implanted stifle.

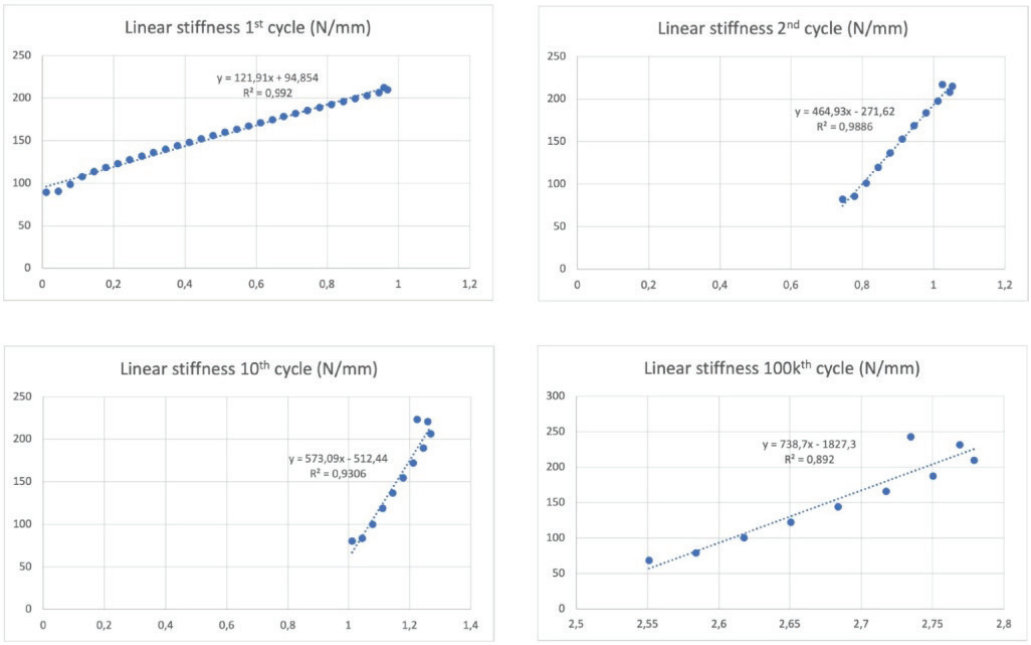

Fig. 5. Linear stiffness at 1st, 2nd, 10th, and 100,000th cycles for the 1D sample.

shape with two major quasi-linear parts. The two parts of the curves were linearly interpolated and these two asymptotes intersected at an average time of 27 minutes. The first phase until 27 minutes corresponds to the main increase in the observed displacement. The second phase corresponds to a slight increasing displacement observable from T = 10 hours until the end of the experiment.

The first cycle of tensile loading (from 100 to 210 N) led to variable linear stiffness between samples: mean = 196 N/mm and standard deviation (SD) = 161 N/mm (Table 1). The linear stiffnesses from this first mechanical traction corresponded to a preloading phase and were therefore not considered later on. Linear stiffnesses calculated at the 2nd, 10th, and 100,000th cycles were quite similar between samples (SD = 90, 70, and 73 N/mm at the 2nd, 10th, and 100,000th cycles, respectively). The displacement recorded at the end of the tests was within the range (0.72–4 mm) (mean = 2.2 mm; SD 1.15 mm). Two samples (1G and 4G) out of the seven exceeded a displacement of 3 mm: this threshold could be chosen as the *in situ* functionality range limit for the fixation system according to previous studies (Loutzenheiser *et al.*, 1995; Wüst *et al.*, 2006).

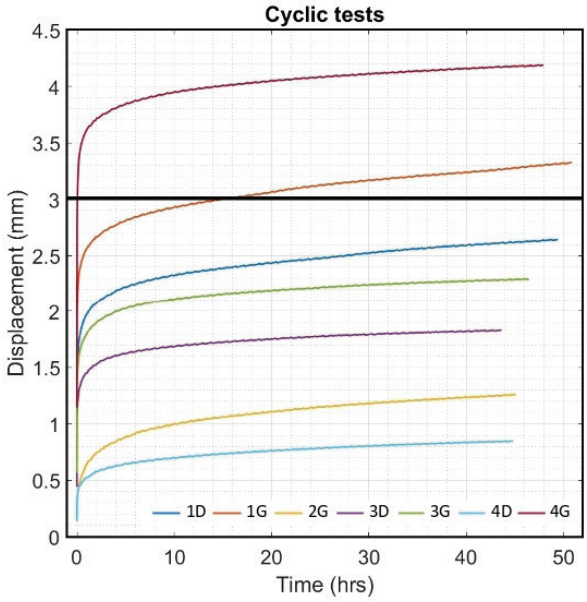

Fig. 6. Evolution over time (hour) of mean filtered displacement (mm) recorded for seven biomechanical cyclic tests. Interval (0–3 mm) of *in situ* functionality of fixation system reported by Wust and Filbert (Loutzenheiser *et al.*, 1995; Wüst *et al.*, 2006) displayed as a horizontal black line.

The linear stiffnesses after the first cycle seem homogeneous throughout the datasets, showing a strong dynamic strength of interference screw-based fixations of the UHMWPE implant in the femoral and tibial bones.

A radiographic control (4G sample) showed a deviation of the implantation axes of the interference screws, which are related to the biomechanical behavior of the UHMWPE implant in the femoral bone tunnels (Fig. 7).

Regarding the data from the seven samples, the nonparametric statistical tests (Kruskal–Wallis H test, Mood's median test, and Levene's test) failed to reject their respective null hypothesis (i.e., that samples came from the same distribution, with an equal median or an equal variance). However, there was insufficient evidence to support the alternative hypothesis, as there was no significant difference between samples. Kendall's coefficient of concordance thus revealed a significant agreement between samples (p = 0.000105). On the contrary, the nonparametric statistical tests (Kruskal–Wallis H test, Mood's median test, and Levene's test) underlined significative differences regarding the stiffness computed at four different loading cycles (p = 3.639e-5, p = 0.000866, p = 0.031161, respectively). The unpaired Mann–Whitney U test showed significant differences in stiffness between cycle 1 and the other

Table 1. Mean and standard deviation (SD) values of linear stiffness calculated from 1st, 2nd, 10th, and 100,000th mechanical traction, and end displacement recorded for each test for validated and slipped samples.

Sample name		Linear stiffness 1st cycle (N/mm)	Linear stiffness 2nd cycle (N/mm)	Linear stiffness 10th cycle (N/mm)	Linear stiffness 100kth cycle (N/mm)	End displacement recorded (mm)
Validated samples	1D	122	465	573	739	2.5
	2G	425	642	733	818	1.1
	3D	116	481	605	824	2.2
	3G	151	511	612	867	1.7
	4D	428	657	728	892	0.72
Slipped samples	1G	79	432	560	680	3.2
	4G	50	474	635	796	4
Mean		196	523	635	802	2.2
SD		161	90	70	73	1.15

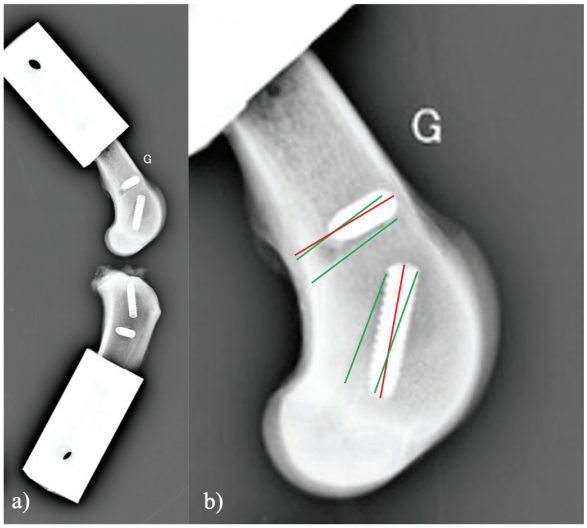

Fig. 7. Profile radiographic control performed after biomechanical test no. 4G: (a) implanted femur and tibia; and (b) zoom on femur distal epiphysis. Green straight lines show tunnel margins. Red straight lines show insertion axis of interference screws. Femoral screws not correctly oriented according to surgical technique recommended by manufacturer.

three cycles (p = 0.000583 for all), between cycle 2 and cycle 100,000 (p = 0.000583), and between cycle 10 and cycle 100,000 (p = 0.002331). The stiffness computed at cycle 100,000 was therefore statistically different from the other three. However, Kendall's coefficient of concordance revealed a significant agreement among the stiffness computed at all four cycles (p = 1.623e-5): the stiffness at cycle 100,000 was quite predictable by using a linear regression based on the three other stiffnesses (p = 0.0251; adj R^2 = 87.8%):

$$K_{100,000} = -329.43 - 1.84 \times K_1 + 5.34 \times K_2 - 2.05 \times K_{10}$$

with K_1, K_2, K_{10}, and $K_{100,000}$ being the stiffness computed at cycles 1, 2, 10, and 100,000, respectively.

Discussion

In this *ex vivo* study, a novel passive fixation technique for the treatment of CCL rupture in mature dogs was evaluated biomechanically. The dynamic behavior of implanted dog stifles was assessed through seven samples under cyclic tensile loading (Fig. 6).

The literature review on *ex-vivo* biomechanical veterinary studies published on passive stabilization techniques for deficient stifles revealed limited research with very different testing protocols (Sicard *et al.*, 2002; Banwell *et al.*, 2005; Burgess *et al.*, 2010; Tonks *et al.*, 2010; Cabano *et al.*, 2011; Rose *et al.*, 2011; Choate *et al.*, 2013; Oda *et al.*, 2016).

Two categories of studies should be distinguished: on the one hand, mechanical studies on the intrinsic mechanical strength of various types of extra-articular suture material (FiberWire, FiberTape, OrthoFiber, etc.), their fixation technique (Knotted, Crimped, etc.), or the effect of the sterilization method use for the suture material (Sicard *et al.*, 2002; Banwell *et al.*, 2005; Burgess *et al.*, 2010; Cabano *et al.*, 2011; Rose *et al.*, 2011); on the other hand, biomechanical studies on the various passive stabilization techniques for deficient stifles using different types of material and fixation systems on cadaveric canine hind limbs (Tonks *et al.*, 2010; Choate *et al.*, 2013; Oda *et al.*, 2016). Therefore, the study published by Choate *et al.* (2013) is the only one that deals with a similar subject and allows a general comparison with our work.

Choate *et al.*'s (2013) publication reporting the *ex vivo* biomechanical characterization (under dynamic loading) of four passive stifle stabilization approaches: nylon leader lateral circumfabellar-tibial suture, FiberTape lateral circumfabellar-tibial suture, TR, and bone anchor. In their study, Choate *et al.* (2013) recorded a maximum displacement ranging from 7.8 to 11.7 mm, corresponding to dynamic traction loads between 80 and 160 N for a maximum of 31,037 cycles. The maximum displacement at the end of our experiments was always lower than their values, despite more loading cycles with a larger amplitude (Fig. 6). Choate *et al.* (2013) respected the physiological angulation of the stifle joint, while the articulation was at 180° in the present study. However, without information on screw angular position in Choate *et al.* (2013), it is impossible to identify which joint configuration induces more pull-out force in the screws close to the ligament.

Two out of our seven samples presented a displacement exceeding the functional threshold of 3 mm (Loutzenheiser *et al.*, 1995; Wüst *et al.*, 2006) at the end of the dynamic loading (1G = 3.2 mm, 4G = 4 mm) and could thus be qualified as "defective" in this context (Loutzenheiser *et al.*, 1995; Wüst *et al.*, 2006). Importantly, *ex vivo* experimentations differ considerably from the physiological reality. In this study, the biomechanical protocol simulated a worse-case condition where the synthetic ligament supports all mechanical loadings. In *in situ* conditions, such loadings are normally distributed between collateral ligaments, CCL, meniscus, and muscles, which also play a major role in the global dynamics of the stifle and in postoperative joint stabilization (Cook, 2010; Kishi *et al.*, 2013; Raske and Hulse, 2013).

The linear regression slope in the second part of all our curves is very gentle (and probably due to a progressive reorganization and orientation of the fibers limited by friction) (Boisse *et al.*, 2001). The number of cycles required to exceed the functional threshold is therefore highly related to the displacement reached at the end of the first period. Pre-tensioning at the beginning of the test was controlled from the loading cell to be similar for each sample. The pre-strain within the ligament was thus almost identical for all samples reconstructed with the same medical device (same material, same weaving pattern, and same geometrical section). One hypothesis

is that the displacement reached after the first period could be related to the initial length of the artificial ligament between samples (which was not quantified, the effective initial length being fixed to anatomical and surgical conditions). The corollary is that this first displacement could be reduced by pre-tensioning during ligament insertion.

The repeatability of experimental conditions is assessed by examining the homogeneity of the results (i.e., low standard deviation values for all computed parameters) (Table 1). These values are in agreement with the final displacement recorded at the end of each test. The two tests (1G and 4G) reporting a lower linear rigidity during the first traction (50 and 79 N/mm) are also the tests which exceeded the functional interval (0–3 mm) (Loutzenheiser *et al.*, 1995; Wüst *et al.*, 2006) of the fixation system with recorded displacements of 3.2 and 4 mm, respectively. Two reasons may explain the specific results observed for these two samples: (i) poor bone quality leading to implant slippage at the bone–screw interface (bone quality was not checked and specimen age was unknown due to anonymized donation); and (ii) incorrect screw orientation despite a good drilling, either during implantation or related to progressive movement due to biomechanical cycling. The posttest X-ray control of the 3G set-up is shown in Figure 7 and highlights a wrong axis of the interference screws in the transversal (angular error of 7°) and oblique (angular error of 9.4°) femur tunnels. Axis alignment errors were also observed in the 1G set-up. It is well known that the trabecular bone is not dense enough to ensure the alignment of the screw with the correct drilling axis and it does not offer the same stiffness as cortical bone to prevent the implant from moving. For future cycling tests, we thus suggest performing an immediate postimplantation X-ray in order to check the initial implantation and any implant movement during cycling, in addition to the posttest X-ray we carried out. The modification of boundary conditions during cycles (from the orientation of the plots) and the displacement of the extremity of the implant (directly on the extreme interference screws by optical measurement) could improve the quantification and the understanding of the mechanisms involved in the slippage of the implant. However, such additional measurements require optical devices that would make the protocol much more demanding in terms of storing and postprocessing computational resources, especially for long cycling tests. Optical measurement is also not compatible with the moistened compresses wrapping the sample.

Our study has some limitations, such as the biomechanical evaluation of a single technique for synthetic reconstruction of the CCL. We are aware that a comparison would have added significant scientific value, but many parameters should be considered when setting up such an experimental protocol.

As with any new surgical technique, a surgeon's learning curve is long in terms of clinical practice and implantation of anatomical parts. Potential biases or diverging interpretations of biomechanical results between surgical techniques should be highlighted. They may concern the material, the braiding and weaving technique, the size and geometry of the synthetic implant, the design and size of interference screws or other fixation systems such as the spiked washer (Barnhart *et al.*, 2019), the size of drill holes made, etc. We precisely chose not to compare our technique of synthetic reconstruction of the CCL to limit these potential biases.

We decided not to test a control group with an intact CCL. Only quasi-static biomechanical tests report the testing of a control group in their experimental protocol (Yoshiya *et al.*, 1986; Flynn *et al.*, 1994; Baltzer *et al.*, 2001; Milano *et al.*, 2006; Sawyer *et al.*, 2012; Biskup *et al.*, 2015). To our knowledge, no study evaluating the biomechanical properties of the fixation system used for intra-articular reconstruction of the CCL in canine cadaver models (or ACL in human cadaver models) by cyclic loading test has made a comparison with a control group of intact *ex vivo* CCLs or ACLs. The duration of the cyclic loading tests reported here (around 50 hour per test) is also drastically longer than in other studies on the characterization of both human and animal fatigue (Nakano *et al.*, 2000; Scheffler *et al.*, 2002; Brown *et al.*, 2004; Spranklin *et al.*, 2006; Choate *et al.*, 2013; Robert *et al.*, 2015; Barnhart *et al.*, 2019; Scannell *et al.*, 2015a, 2015b).

Intra-articular length of the synthetic implant was not measured after implantation, nor was it during the tests. This information is necessary to compute the strain produced by fatigue loadings and should be included in future studies.

The small differences in mean linear stiffness observed in all the tests clearly show that the stiffness of the UHMWPE implant fixed with four interference screws does not vary significantly across dynamic biomechanical loadings (Loutzenheiser *et al.*, 1995; Wüst *et al.*, 2006). An implantation error may have occurred in the two nonvalidated set-ups, thus underlining the importance of the learning curve specific to each surgical technique to obtain optimal results. Our findings show that the technique assessed in this study leads to good performances, which should revive interest in intra-articular reconstruction after CCL rupture in dogs.

Conclusion

The present findings show that the use of four interference screws as a fixation system for a UHMWPE implant leads to satisfactory cyclic pull-out strength compatible with synthetic CCL reconstruction for dogs, from both a biomechanical and *ex vivo* point of view. These results underline the value of intra-articular reconstruction after CCLr in dogs. Additional *in vivo* studies are needed to determine the clinical outcomes of this technique in the postoperative period.

Data availability

All the data are presented in tables or figures directly in this article.

Conflicts of interest

The authors have no conflicts of interest to declare.

Funding statement

This study was supported by the company Novetech Surgery, which provided human resources in the person of Bastien Goin for data processing and writing of this scientific article during his thesis.

Acknowledgments

The authors thank Mrs. Cooke-Martageix for English copyediting of this article.

References

Baird, D.K., Hathcock, J.T., Kincaid, S.A., Rumph, P.F., Kammermann, J., Widmer, W.R., Visco, D. and Sweet, D. 1998. Low-field magnetic resonance imaging of early subchondral cyst-like lesions in induced cranial cruciate ligament deficient dogs. Vet. Radiol. Ultrasound 39(3), 167–173.

Baltzer, W.I., Schulz, K.S., Stover, S.M., Taylor, K.T. and Kass, P.H. 2001. Biomechanical analysis of suture anchors and suture materials used for toggle pin stabilization of hip joint luxation in dogs. Am. J. Vet. Res. 62(5), 721–728.

Banwell, M.N., Kerwin, S.C., Hosgood, G., Hedlund, C.S. and Metcalf, J.B. 2005. *In vitro* evaluation of the 18 and 36 kg securos cranial cruciate ligament repair system. Vet. Surg. 34(3), 283–288.

Barnhart, M., Bufkin, B. and Litsky, A. 2019. Biomechanical comparison of four methods of fixation of a polymeric cranial cruciate ligament in the canine femur and tibia. Vet. Comp. Orthop. Traumatol. 32(2), 112–116.

Barnhart, M.D., Getzy, D. and Gardiner, D.W. 2018. Histologic analysis of retrieved synthetic ligaments implanted in dogs for treatment of cranial cruciate ligament disease. J. Vet. Sci. Med. Diagn. 07(1); doi:10.4172/2325-9590.1000248.

Barnhart, M.D., Maritato, K., Schankereli, K., Wotton, H. and Naber, S. 2016. Evaluation of an intra-articular synthetic ligament for treatment of cranial cruciate ligament disease in dogs: a six-month prospective clinical trial. Vet. Comp. Orthop. Traumatol. 29(6), 491–498.

Biskup, J.J., Balogh, D.G., Haynes, K.H., Freeman, A.L. and Conzemius, M.G. 2015. Mechanical strength of four allograft fixation techniques for ruptured cranial cruciate ligament repair in dogs. Am. J. Vet. Res. 76(5), 411–419.

Biskup, J.J. and Conzemius, M.G. 2020. Long-term arthroscopic assessment of intra-articular allografts for treatment of spontaneous cranial cruciate ligament rupture in the dog. Vet. Surg. 49(4), 764–771.

Blanc, Q., Goin, B., Rafael, P., Moissonnier, P., Carozzo, C., Buttin, P., Cachon, T. and Viguier, E. 2019. Effect of the number of interference screws for the fixation of an intra-articular cranial cruciate ligament prosthesis in dogs: Biomechanical study. Comput. Methods Biomech. Biomed. Eng. 22(suppl. 1), S102–S104.

Boisse, P., Gasser, A. and Hivet, G. 2001. Analyses of fabric tensile behaviour: determination of the biaxial tension–strain surfaces and their use in forming simulations. Compos. Part. A Appl. Sci. Manuf. 32(10), 1395–1414.

Brown, C.H., Wilson, D.R., Hecker, A.T. and Ferragamo, M. 2004. Graft-bone motion and tensile properties of hamstring and patellar tendon anterior cruciate ligament femoral graft fixation under cyclic loading. Arthrosc. J. Arthrosc. Relat. Surg. 20(9), 922–935.

Burgess, R., Elder, S., McLAUGHLIN, R. and Constable, P. 2010. *In vitro* biomechanical evaluation and comparison of FiberWire, FiberTape, OrthoFiber, and nylon leader line for potential use during extra articular stabilization of canine cruciate deficient stifles. Vet. Surg. 39(2), 208–215.

Butler, D.L., Hulse, D.A., Kay, M.D., Grood, E.S., Shires, P.K., D'Ambrosia, R. and Shoji, H. 1983. Biomechanics of cranial cruciate ligament reconstruction in the dog II. Mechanical properties. Vet. Surg. 12(3), 113–118.

Cabano, N.R., Troyer, K.L., Palmer, R.H., Puttlitz, C.M. and Santoni, B.G. 2011. Mechanical comparison of two suture constructs for extra-capsular stifle stabilization: mechanical comparison of suture constructs. Vet. Surg. 40(3), 334–339.

Choate, C.J., Lewis, D.D., Conrad, B.P., Horodyski, M.B. and Pozzi, A. 2013. Assessment of the craniocaudal stability of four extracapsular stabilization techniques during two cyclic loading protocols: a cadaver study: cyclic loading of extra capsular techniques. Vet. Surg. 42(7), 853–859.

Cocca, C.J., Duffy, D.J., Kersh, M.E. and Moore, G.E. 2020. Influence of interlocking horizontal mattress epitendinous suture placement on tendinous biomechanical properties in a canine common calcaneal laceration model. Vet. Comp. Orthop. Traumatol. 33(3), 205–211.

Cook, J., Smith, P., Stannard, J., Pfeiffer, F., Kuroki, K., Bozynski, C. and Cook, C. 2017. A canine arthroscopic anterior cruciate ligament reconstruction model for study of synthetic augmentation of tendon allografts. J. Knee Surg. 30(7), 704–711.

Cook, J.L. 2010. Cranial cruciate ligament disease in dogs: biology versus biomechanics: biology versus biomechanics. Vet. Surg. 39(3), 270–277.

Cook, J.L., Luther, J.K., Beetem, J., Karnes, J. and Cook, C.R. 2010. Clinical comparison of a novel extracapsular stabilization procedure and tibial plateau leveling osteotomy for treatment of cranial

cruciate ligament deficiency in dogs: TightRope for CCL in dogs. Vet. Surg. 39(3), 315–323.

FLO, G.L. 1975. Modification of the lateral retinacular imbrication technique for stabilizing cruciate ligament injuries. JAAHA 11, 570–576.

Flynn, M.F., Edmiston, D.N., Roe, S.C., Richardson, D.C., Deyoung, D.J. and Abrams, CF. 1994. Biomechanical evaluation of a toggle pin technique for management of coxofemoral luxation. Vet. Surg. 23(5), 311–321.

Gao, K., Chen, S., Wang, L., Zhang, W., Kang, Y., Dong, Q., Zhou, H. and Li, L. 2010. Anterior cruciate ligament reconstruction with LARS artificial ligament: a multicenter study with 3- to 5-year follow-up. Arthrosc. J. Arthrosc. Relat. Surg. 26(4), 515–523.

Goin, B., Rafael, P., Blanc, Q., Cachon, T., Buttin, P., Carozzo, C., Chabrand, P. and Viguier, E. 2019. Biomechanical analysis of a ligament fixation system for CCL reconstruction in a canine cadaver model. Comput. Methods Biomech. Biomed. Eng. 22(suppl. 1), S109–S111.

Hui, C., Salmon, L.J., Kok, A., Maeno, S., Linklater, J. and Pinczewski, L.A. 2011. Fifteen-year outcome of endoscopic anterior cruciate ligament reconstruction with patellar tendon autograft for "isolated" anterior cruciate ligament tear. Am. J. Sports Med. 39(1), 89–98.

Johnson, J.M. and Johnson, A.L. 1993. Cranial cruciate ligament rupture: pathogenesis, diagnosis, and postoperative rehabilitation. Vet. Clin. North Am. Small Anim. Pract. 23(4), 717–733.

Kim, S.E., Pozzi, A., Kowaleski, M.P. and Lewis, D.D. 2008. Tibial osteotomies for cranial cruciate ligament insufficiency in dogs. Vet. Surg. 37(2), 111–125.

Kishi, E.N., Hulse, D., Raske, M., Saunders, W.B. and Beale, B.S. 2013. Extra-articular stabilization of the canine cranial cruciate ligament injury using arthrex corkscrew and FASTak anchors. Open J. Vet. Med. 3(2), 156–160.

Kousa, P., Järvinen, T.L.N., Vihavainen, M., Kannus, P. and Järvinen, M. 2003. The fixation strength of six hamstring tendon graft fixation devices in anterior cruciate ligament reconstruction: part I: femoral site. Am. J. Sports Med. 31(2), 174–181.

Legnani, C., Ventura, A., Terzaghi, C., Borgo, E. and Albisetti, W. 2010. Anterior cruciate ligament reconstruction with synthetic grafts. A review of literature. Int. Orthop. 34(4), 465–471.

Loutzenheiser, T.D., Harryman, D.T., Yung, S.-W., France, M.P. and Sidles, J.A. 1995. Optimizing arthroscopic knots. Arthrosc. J. Arthrosc. Relat. Surg. 11(2), 199–206.

Milano, G., Mulas, P.D., Ziranu, F., Piras, S., Manunta, A. and Fabbriciani, C. 2006. Comparison between different femoral fixation devices for ACL reconstruction with doubled hamstring tendon graft: a biomechanical analysis. Arthrosc. J. Arthrosc. Relat. Surg. 22(6), 660–668.

Nakano, H., Yasuda, K., Tohyama, H., Yamanaka, M., Wada, T. and Kaneda, K. 2000. Interference screw fixation of doubled flexor tendon graft in anterior cruciate ligament reconstruction—biomechanical evaluation with cyclic elongation. Clin. Biomech. 15(3), 188–195.

Oda, S.G.S., Souza, A.N.A., Pereira, C.A.M., Escobar, A.S.A., Tartarunas, A.C. and Matera, J.M. 2016. Biomechanical evaluation of two extracapsular techniques for cranial cruciate ligament reconstruction in cadaver dogs. Semina. Ciênc. Agrár. 37(3), 1327.

Patterson, R.H., Smith, G.K., Gregor, T.P. and Newton, C.D. 1991. Biomechanical stability of four cranial cruciate ligament repair techniques in the dog. Vet. Surg. 20(2), 85–90.

Prada, T.C., Silva, A.C. and da Minto, B.W. 2018. Short-term evaluation of an intra-articular technique for cranial cruciate ligament rupture in dogs using nylon or polyester. Semina. Ciênc. Agrár. 39(2), 593.

Rafael, P., Goin, B., Buttin, P., Cachon, T. and Viguier, E. 2020. Comparison of two methods of fixation with interference screw for cranial cruciate ligament reconstruction in canine cadaver model. Comput. Methods Biomech. Biomed. Eng. 23(suppl. 1), S247–S249.

Raske, M. and Hulse, D. 2013. SwiveLock bone anchor stabilization of the cranial cruciate ligament deficient stifle in dogs: clinical outcome. Open J. Vet. Med. 3(7), 297–301.

Robert, H., Bowen, M., Odry, G., Collette, M., Cassard, X., Lanternier, H. and De Polignac, T. 2015. A comparison of four tibial-fixation systems in hamstring-graft anterior ligament reconstruction. Eur. J. Orthop. Surg. Traumatol. 25(2), 339–347.

Rose, N.D., Goerke, D., Evans, R.B. and Conzemius, M.G. 2011. Mechanical testing of orthopedic suture material used for extra-articular stabilization of canine cruciate ligament-deficient stifles: mechanical testing of orthopedic suture material. Vet. Surg. 41(2), 266–272.

Rumph, P.F., Kincaid, S.A., Visco, D.M., Baird, D.K., Kammermann, J.R. and West, M.S. 1995. Redistribution of vertical ground reaction force in dogs with experimentally induced chronic hindlimb lameness. Vet. Surg. 24(5), 384–389.

Salmon, L.J., Russell, V.J., Refshauge, K., Kader, D., Connolly, C., Linklater, J. and Pinczewski, L.A. 2006. Long-term outcome of endoscopic anterior cruciate ligament reconstruction with patellar tendon autograft: minimum 13-year review. Am. J. Sports Med. 34(5), 721–732.

Sawyer, G., Anderson, B., Paller, D., Heard, W. and Fadale, P. 2012. Effect of interference screw

fixation on ACL graft tensile strength. J. Knee Surg. 26(3), 155–160.

Scannell, B.P., D'Alessandro, D.F., Connor, P.M. and Fleischli, J.E. 2015a. Biomechanical comparison of hamstring tendon fixation devices for anterior cruciate ligament reconstruction: part 1. five femoral devices. Am. J. Orthop. (Belle Mead NJ) 44(1), 32–36.

Scannell, B.P., D'Alessandro, D.F., Connor, P.M. and Fleischli, J.E. 2015b. Biomechanical comparison of hamstring tendon fixation devices for anterior cruciate ligament reconstruction: part 2. four tibial devices. Am. J. Orthop. (Belle Mead NJ) 44(2), 82–85.

Scheffler, S.U., Südkamp, N.P., Göckenjan, A., Hoffmann, R.F.G. and Weiler, A. 2002. Biomechanical comparison of hamstring and patellar tendon graft anterior cruciate ligament reconstruction techniques. Arthrosc. J. Arthrosc. Relat. Surg. 18(3), 304–315.

Sicard, G.K., Hayashi, K. and Manley, P.A. 2002. Evaluation of 5 types of fishing material, 2 sterilization methods, and a crimp-clamp system for extra-articular stabilization of the canine stifle joint. Vet. Surg. 31(1), 78–84.

Spranklin, D., Elder, S., Boyle, C. and McLaughlin, R. 2006. Comparison of a suture anchor and a toggle rod for use in toggle pin fixation of coxofemoral luxations. J. Am. Anim. Hosp. Assoc. 42(2), 121–126.

Tonks, C.A., Pozzi, A., Ling, H.Y. and Lewis, D.D. 2010. The effects of extra-articular suture tension on contact mechanics of the lateral compartment of cadaveric stifles treated with the TightRope CCL® or lateral suture technique: contact pressures after extra-articular stabilization. Vet. Surg. 39(3), 343–349.

von Pfeil, D.J.F., Kowaleski, M.P., Glassman, M. and Dejardin, L.M. 2018. Results of a survey of Veterinary Orthopedic Society members on the preferred method for treating cranial cruciate ligament rupture in dogs weighing more than 15 kilograms (33 pounds). J. Am. Vet. Med. Assoc. 253(5), 586–597.

Wilke, V.L., Robinson, D.A., Evans, R.B., Rothschild, M.F. and Conzemius, M.G. 2005. Estimate of the annual economic impact of treatment of cranial cruciate ligament injury in dogs in the United States. J. Am. Vet. Med. Assoc. 227(10), 1604–1607.

Witsberger, T.H., Villamil, J.A., Schultz, L.G., Hahn, A.W. and Cook, J.L. 2008. Prevalence of and risk factors for hip dysplasia and cranial cruciate ligament deficiency in dogs. J. Am. Vet. Med. Assoc. 232(12), 1818–1824.

Wüst, D.M., Meyer, D.C., Favre, P. and Gerber, C. 2006. Mechanical and handling properties of braided polyblend polyethylene sutures in comparison to braided polyester and monofilament polydioxanone sutures. Arthrosc. J. Arthrosc. Relat. Surg. 22(11), 1146–1153.

Yoshiya, S., Andrish, J.T., Manley, M.T. and Kurosaka, M. 1986. Augmentation of anterior cruciate ligament reconstruction in dogs with prostheses of different stiffnesses. J. Orthop. Res. 4(4), 475–485.